ISSN: 2633-4828 Vol. 5 No.1, January, 2023

International Journal of Applied Engineering & Technology

EFFECT OF REACTION TIME ON THE PROPERTIES OF SnO_2 NANOPARTICLES

J. Priya Sharon[1], K. Gnanaprakasam Dhinakar[2*]

[1]Research Scholar and [2*]Assistant Professor, PG & Research Department of Physics, Pope's College (Autonomous), Sawyerpuram – 628 251, Tamil Nadu, India

[1, 2]Affiliated to Manonmaniam Sundaranar University, Abishekapatti, Tirunelveli – 627 012, Tamil Nadu, India

[2*]kdhinakarr@gmail.com

ABSTRACT

SnO_2 nanoparticles are synthesized using a solvothermal method at the temperature of 200°C with different reaction time (3 & 6 hours) and annealed at 500°C for 1 hour. The obtained XRD pattern reveals that the nanoparticles are in tetragonal crystal structure and the XRD data is well matched with JCPDS card no 077-0447. The average particle size is calculated using Sherrer's formula as 23nm and 27nm. SEM images inferred that the particles are in spherical shape. EDAX results confirms the presence of Sn and O. FTIR spectroscopy was used to establish the functional groups present in the obtained nanoparticles. The optical bandgap of the two different SnO2 nanoparticles were calculated as 3.56eV and 2.98eV respectively using Tauc plot. Grain-dominated conduction behavior, frequency-dependent dielectric dispersion, and increased AC conductivity at higher frequencies were all shown by impedance and dielectric investigations. The findings show that SnO_2 nanoparticles' physical characteristics may be tuned for possible optoelectronic and energy-related applications by adjusting their reaction time.

Keywords: *tin dioxide; solvothermal synthesis; nanoparticles; characterization; impedance spectroscopy*.

1. INTRODUCTION

Owing to their long cycle life, low cost, and high theoretical capacitance, transition metal oxides are used in energy storage applications (as redox material). Some specific transition metal oxides which was extensively explored are: tin oxide (SnO_2), tungsten oxide (WO_3), vanadium pentoxide (V_2O_5), manganese dioxide (MnO_2), nickel oxide (NiO)[1].

Because of their superior capacitive properties, transition metal oxides may be classified as noble transition metal oxides[2]. Metal oxide semiconductors have tunable large bandgap and they are highly stable, low cost materials[3] and play a key role in various application like drug and health-related industry[4], (opto)electronic materials, catalysis and environmental remediation[5]. Transition metal oxide nanocomposites are promising for many application uses such as Sensors, Solar Cells, Bactericidal properties, Photocatalytic Degradation, Supercapacitors etc.[6]. There is a lot of energy storage devices are used by researchers, but some of them like supercapacitors, sodium-ion batteries (SIBs) and lithium-ion batteries (LIBs) show outstanding portability, strong independence and environmental friendliness[7,8]. A lot of tin-based composites and its intermetallics shows increased long-term cycling stability compared to metallic Sn when we used as lithium storage materials[9].

Various methods can be carried out to produce highly crystalline SnO_2 nanoparticles like solvothermal method[10, 11], chemical co-precipitation method[12], sol-gel technique[13], hydrothermal method[14], chemical reduction[15] etc. The properties of the material changes by many reasons but one of them is synthesis method. Hydrothermal and solvothermal provides good morphologies and particle size control and environmentally friendly. For improving the functionality of several materials, the hydrothermal or solvothermal processes shows marvelous potential, and it offers many applications such as infrared shielding materials, ultraviolet rays, photocatalysts, non-toxic pigments, and etc.[16].

Tin dioxide (SnO_2) is an n-type semiconductor and it has a vast potential applications in gas sensors[17], transparent electrodes, catalysts, transistors, and batteries[18]. At room temperature, SnO_2 has a wide band gap of 3.6 eV[19]. In virtue of its magnificent properties for instance, great optical and electrical properties, low cost, fast response and

high sensitivity, SnO_2 is the subject of large-scale research development[20]. For perovskite solar cells (PSCs), Tin oxide (SnO_2) has come up as a good electron transport layer[21].

In the present work, the SnO_2 nanoparticles are synthesized at same temperature (200°C) with different reaction time and its structural, morphological, optical and electrical properties were studied.

2. METHODS

2.1 Synthesis of SnO_2 nanoparticles

The precursors used for the synthesis of SnO_2 were Analytical grade Stannous Chloride, Urea as catalyst and Ethylene Glycol as solvent. Tin chloride and urea are taken as solute in the molecular ratio 1:3 and dissolved in 50 ml ethylene glycol and stirred for 1 hour in a magnetic stirrer. Then the prepared solution was moved into a 100 mL Teflon autoclave and maintained at 200 °C for 3 hours and 6 hours. The resulting precipitate was washed with double distilled water, filtered and dried. The obtained powders were washed with acetone. The sample was annealed at 500°C for 1 hour. Finally, the SnO_2 nanoparticles were obtained.

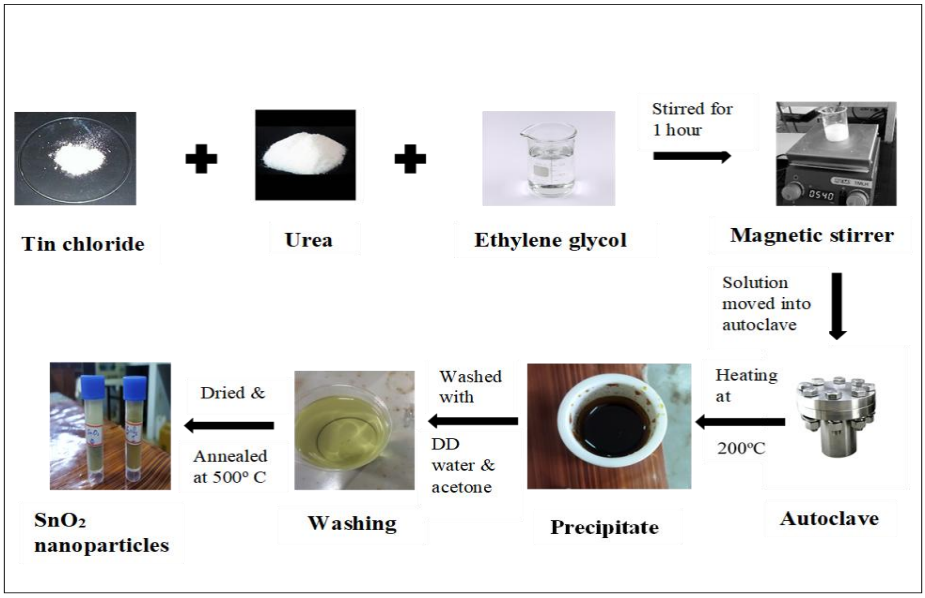

Figure 2.1: Synthesis of SnO_2 nanoparticles

3. RESULTS AND DISCUSSION

3.1 X-Ray Diffraction Pattern Analysis

From the XRD patterns, we can find out the crystalline nature of the synthesized nanoparticles and confirms the formation of tetragonal structure of two different SnO_2 nanoparticles (T1 and T2)[22]. Figure 3.1 indicates the powder XRD patterns of synthesized SnO_2 nanoparticles, it reveals that the obtained particles are in tetragonal crystalline structure.

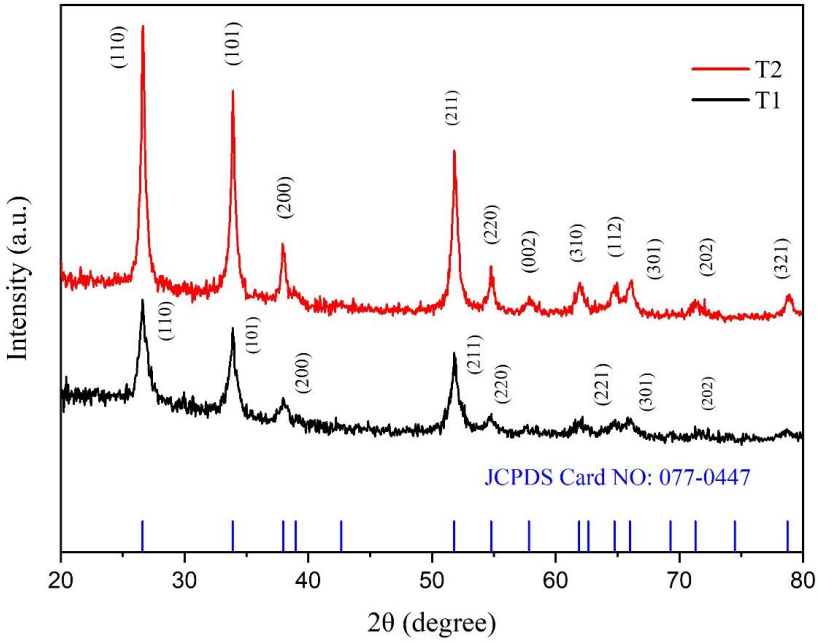

Figure 3.1: The powder XRD patterns of two different SnO2 nanoparticles

The result is well matched with the JCPDS card no.: 077-044723. It infers that the crystallinity of the sample increases with the increase of reaction time. The obtained XRD results of two SnO_2 nanoparticles show that the peaks are resolved well and have good sharpness when increasing the synthesis time[24]. The observed eight diffraction peaks of sample T1 at the 2θ range are 26.63°, 33.92°, 38.12°, 51.8°, 54.76°, 62.06°, 66.13° and 71.71° are ascribed to the miller indices (110), (101), (200), (211), (220), (221), (301), (202). The detected eleven diffraction peak of sample T2 at the angle 2θ range are 26.63°, 33.91°, 37.97°, 51.83°, 54.81°, 57.87°, 61.91°, 64.76°, 66.8°, 71.32°, 78.77° belong to the hkl planes of (110), (101), (200), (211), (220), (002), (310), (112), (301), (202), (321)25,26. Using Bragg's law, the line spacing between two lattice planes are deliberate as follows: $n\lambda = 2dsin\theta$, Where, n is an integer value and d is the distance between two lattice planes[27]. The crystallite size of the two different SnO_2 nanoparticles are found by using Debye Sherrer formula which is given by, $D = k\lambda/(\beta\cos\theta)$, Where k is Sherrer constant, λ is wavelength of X-ray, β is full width at half maximum and θ is Bragg incident angle[28, 29]. The average crystallite size of the samples were arrived as 23nm and 27nm respectively. The average crystallite size and the intensity of the peaks are increased when we increase the reaction time30. The lattice parameters can be calculated by using the formula, $1/d^2 = [(h^2+k^2)/a^2] + l^2/c^2$, Where, h, k, l are miller indices and a, b, c are lattice parameters. The calculated values of a, b, c are 4.73 Å, 4.73 Å and 3.18 Å respectively[29, 31].

3.2. SEM Analysis:

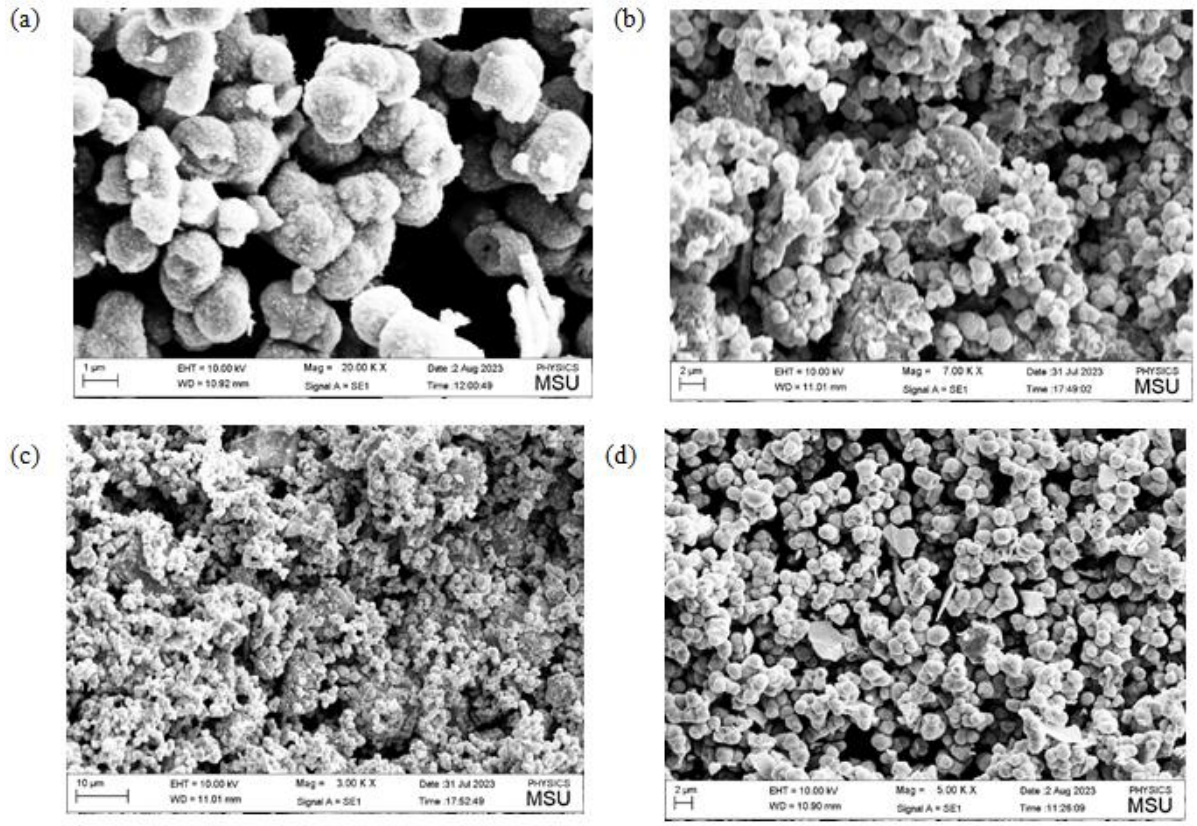

Figure 3.2: a, b are SEM images of sample T1 & c, d are SEM images of sample T2.

The investigation of the surface morphology of the two samples were scrutinized by scanning electron microscopy (SEM). The above figure shows the SEM images of two different SnO_2 nanoparticles. Both type of the particles are agglomerated morphology and having spherical in shape[26, 31, 32].

3.3. EDAX Analysis:

The elemental makeup of the produced SnO_2 nanoparticles was ascertained by Energy Dispersive X-ray Analysis (EDAX). The synthesis of tin dioxide without detectable impurity elements is confirmed by the prominent distinctive peaks that correspond to tin (Sn) and oxygen (O) in the EDAX spectra of both samples (T1&T2). The great purity of the produced nanoparticles and the efficacy of the solvothermal synthesis process are confirmed by the existence of just Sn and O peaks. The peaks' relative intensities indicate that SnO_2 has the right stoichiometric composition. Moreover, the lack of other elemental signals verifies that no impurities or secondary phases were added during synthesis or annealing[22, 33]. As a consequence, the EDAX results validate the successful synthesis of phase-pure SnO_2 nanoparticles and corroborate the XRD findings.

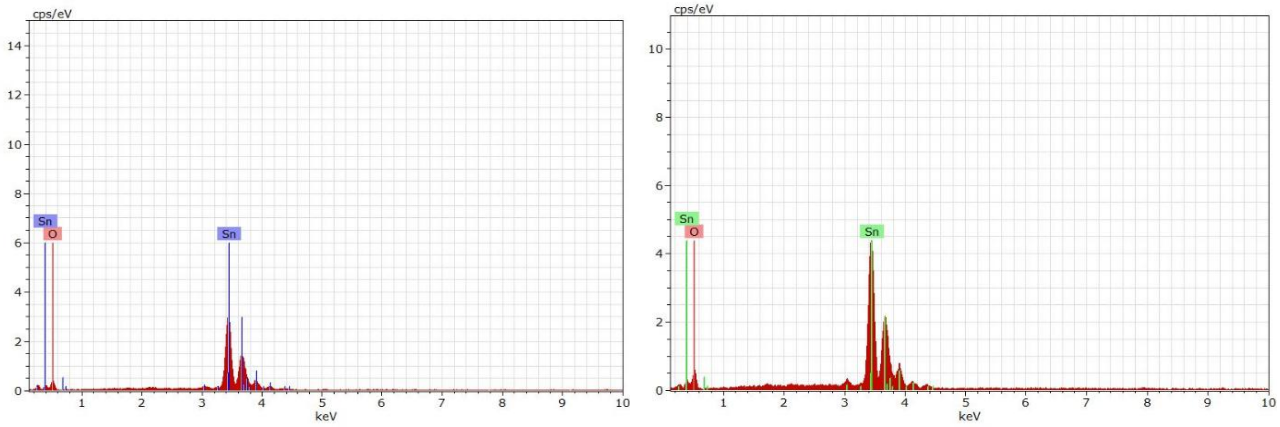

Figure 3.3: The EDAX spectra of two samples T1 & T2.

3.4. FTIR Spectrum Analysis:

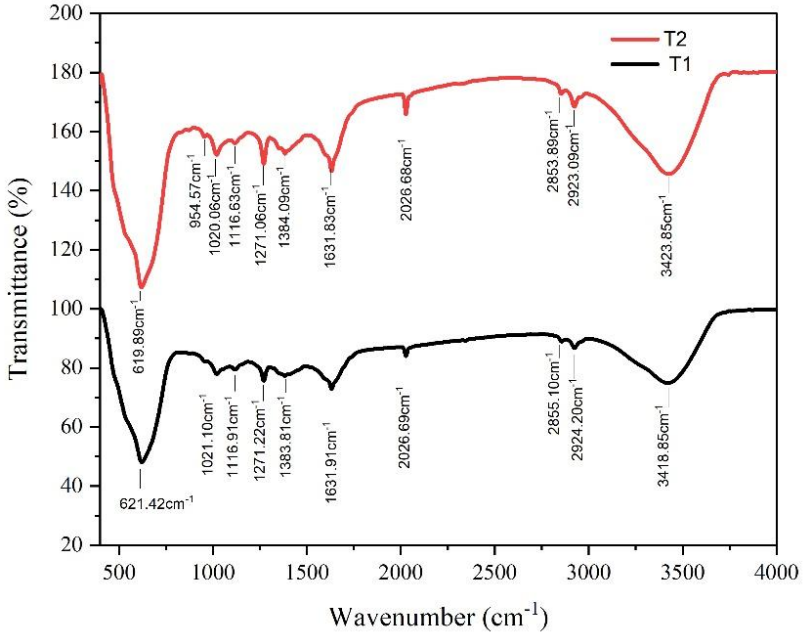

Figure 3.4: The FTIR spectra of two samples T1 & T2.

Figure 3.4 shows the FTIR spectra of the SnO_2 nanoparticles with in the wavelength region ranging from 400cm^{-1}-4000cm^{-1}. From the FTIR spectra, the stretching modes of Sn-O are confirmed by the peaks which falls on 621.42cm^{-1} and 619.89cm^{-1} and the Sn-O stretching vibrations are established in the region ranging from 800-400 cm^{-1}. The observed IR bands of two samples are 3418.85 and 3423.85cm^{-1} marks the O-H stretching and 1631.91 cm^{-1} and 1631.83cm^{-1} O-H bending vibrations of water molecule respectively[24, 34].

3.5. UV-Vis Spectrum Analysis:

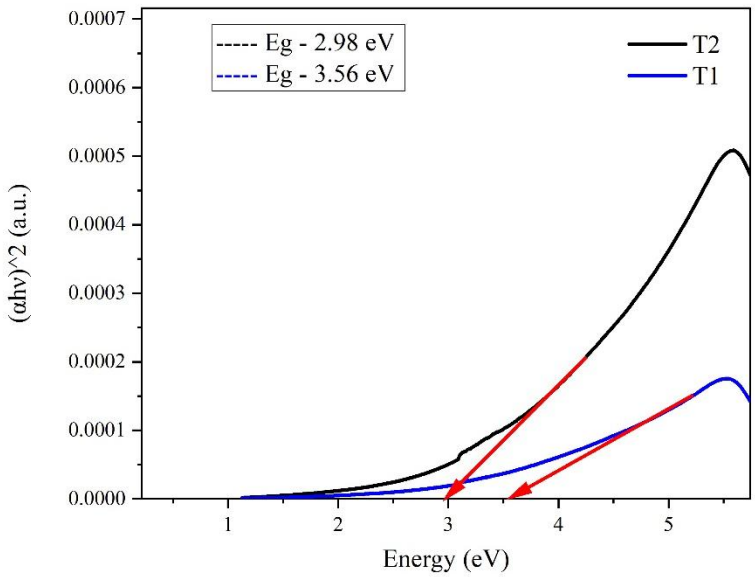

Figure 3.5: Band gap energies of SnO_2 nanoparticle samples T1 & T2.

The UV-Visible spectra recorded in the range of 200 nm to 800 nm. The bandgap of the synthesized SnO_2 nanoparticles are calculated from Tauc plot. Figure 3.5 shows the Tauc plot of SnO_2 nanoparticles with reaction time 6 hours and 3 hours respectively. The calculated bandgap values are 3.56eV and 2.98eV[38]. The absorption coefficient (α) and optical bandgap (Eg) are related in a direct transition semiconductor as:

$$(\alpha h\nu)^2 = \beta\,(h\nu - E_g)$$

Where h is Planck's constant, ν the frequency of incident photon and β is energy independent constant[35, 36]. The absorption coefficient (α) can be studied by the following equation:

$$\alpha = 2.303A/t$$

Where A is the absorbance and t is the width of the cuvette used for taking the sample for measuring the absorbance of the prepared material[37]. The bandgap energy is decreased when the reaction time increased[39].

3.6. Impedance analysis

Room temperature complex impedance spectra was recorded and analyzed to study the electrical behavior of the SnO_2 nanoparticles. The complex impedance (Z'') was then plotted as function of the real part of the impedance (Z') for both sample studied for frequencies ranging from 100 Hz to 10^6 Hz. Figure 3.6.1 shows the Nyquist plot for SnO_2 nanoparticles. Both the spectra exhibit almost semicircle arcs with different sizes specifies that the remarkable benefaction to impedance results from grains[41]. When crystallite size of the sample decreases the radius of the semicircular arcs increases.

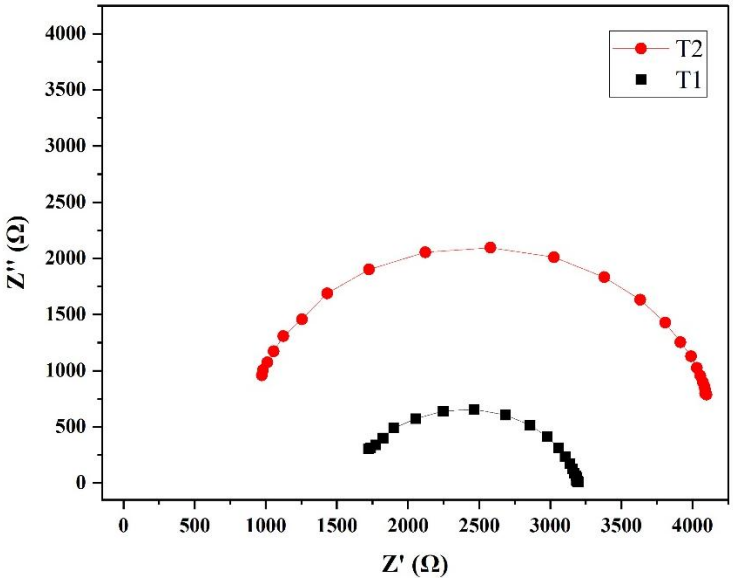

Figure 3.6.1: Impedance spectra of SnO_2 nanoparticle samples T1 & T2.

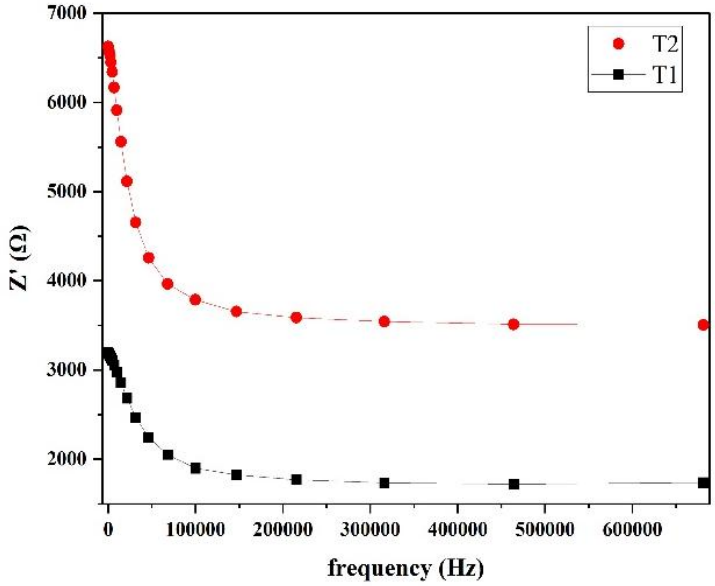

Figure 3.6.2: The plot of frequency vs real part of impedance (Z') of the SnO_2 samples T1&T2.

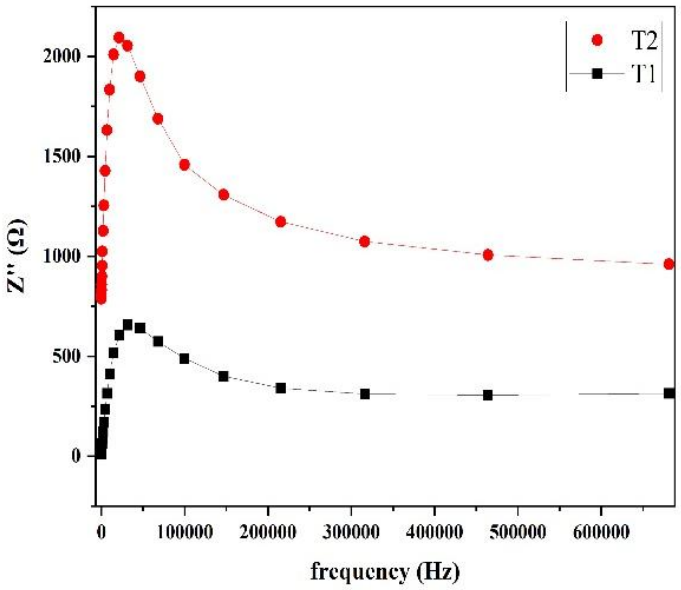

Figure 3.6.3: The plot of frequency vs imaginary part of impedance (Z'') of the SnO_2 samples T1&T2.

Figure 3.6.2 shows the plot of frequency vs real part of impedance (Z'). It shows a dispersive nature at low frequency and attaints constant values at a higher frequency. Z' values are higher in low frequency and have lesser value in high frequency. The decreases of the real value of the impedance (Z') at high frequency is due to increase in ac conductivity for all samples. Fig. 3.6.3 displays the various plots of imaginary vs frequency. Z'' exhibit peaking comportment and reaches a high value and then decrease with increasing frequency[42].

3.7. Dielectric analysis

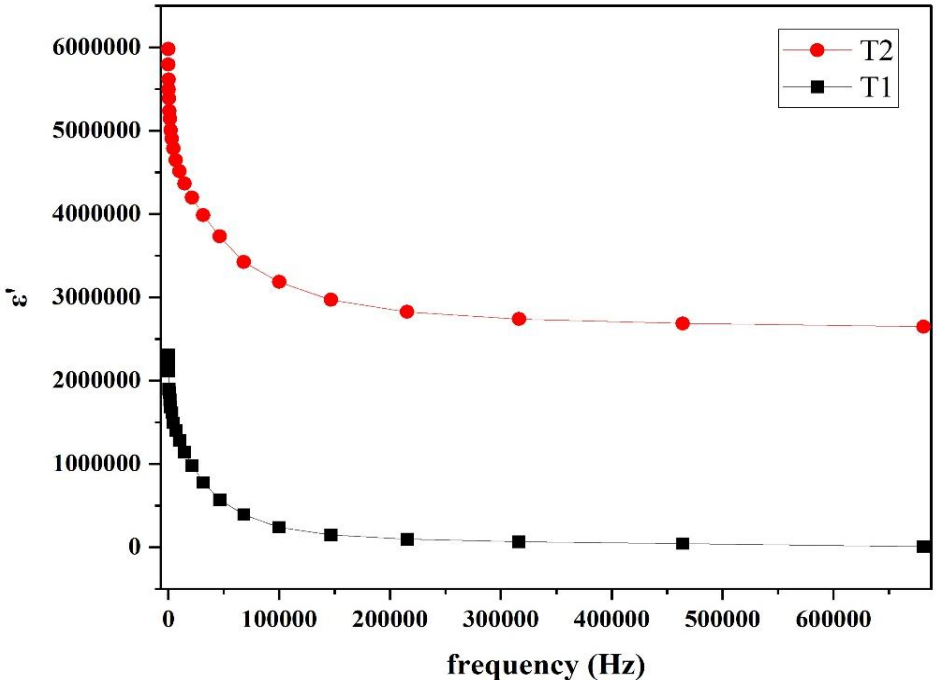

Figure 3.7.1: The dielectric constant of SnO_2 nanoparticles for various frequencies.

Frequency dependence of dielectric constant and loss can explore useful information about structural changes, transport mechanism and defect behavior of a solid. Even the slightest chemical and physical change has a dramatic effect on the dielectric properties. The ratio between ε'' and ε' defines a loss tangent, tan δ = ε''/ε'[43].

Figure 3.7.1 shows the dielectric constant of both the SnO_2 nanoparticles for various frequencies. The real and imaginary parts of the dielectric constants are calculated by using the following equation:

$$\varepsilon' = -Z''/\omega Co(Z'^2 + Z''^2)$$

$$\varepsilon'' = -Z'/\omega Co(Z'^2 + Z''^2)$$

Where, ω is the angular frequency, C_0 is the geometrical capacitance, Z' and Z'' are real and imaginary parts of impedance[44].

At room temperature, the dielectric constant decreases with increase of frequency. At low frequencies, all type of polarizations contribute to the dielectric constant value as deformational polarization and relaxation. The interfacial and orientation polarizations are much important. At high frequency, ε' reached a constant value due to interfacial polarization.

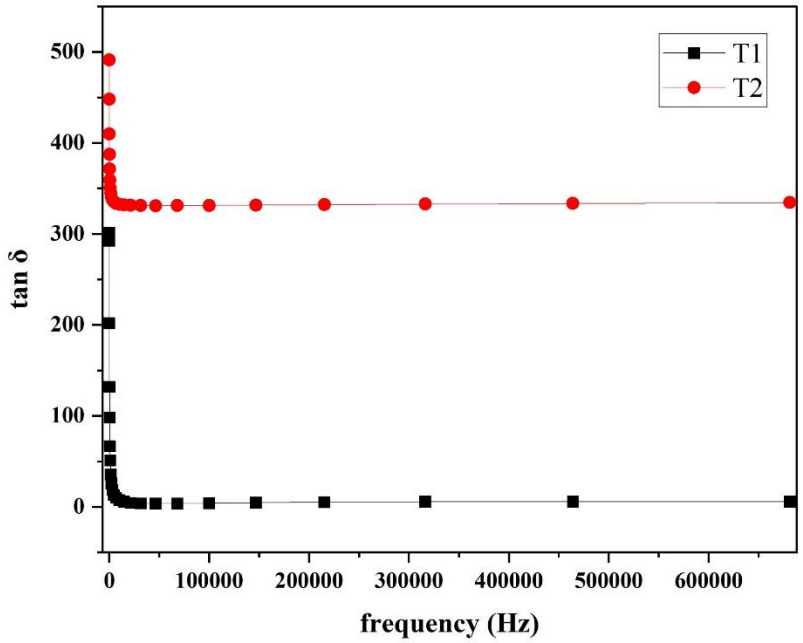

Figure 3.7.2: Frequency vs. tan δ of samples T1 & T2.

The variation of dielectric loss tangent (tan δ) with frequency has shown in figure 3.7.2. Dielectric loss represents the energy dissipation in the dielectric system. At low frequencies, the tan d values are maximum and highly dispersive in nature. It is clearly seen that, an increase in the frequency, decreases the value of dielectric loss factor[45].

3.8. AC conductivity Analysis

The measurement of an AC conductivity is a significant tool for determining the eminent transport properties of materials. The Ac conductivity is assessed using the following equation:

$$\sigma_{ac} = \omega\varepsilon_0\varepsilon'' = 2\pi f\,\varepsilon_0\varepsilon''$$

Where $\omega = 2\pi f$ is the angular frequency and f is the frequency of the applied field, ε_0 is the permittivity of free space, ε'' is the imaginary part of the dielectric constant[44].

Figure shows a typical frequency dependence of ac conductivity σ_{ac} for SnO_2 nanoparticles at room temperature. For both the samples, the ac conductivity increases linearly with the frequency. This shows that the conduction mechanism is correlate with the translational hopping motion[40]. When the frequency is increased the ac conductivity also increases which is ascribed to the series resistance effect.

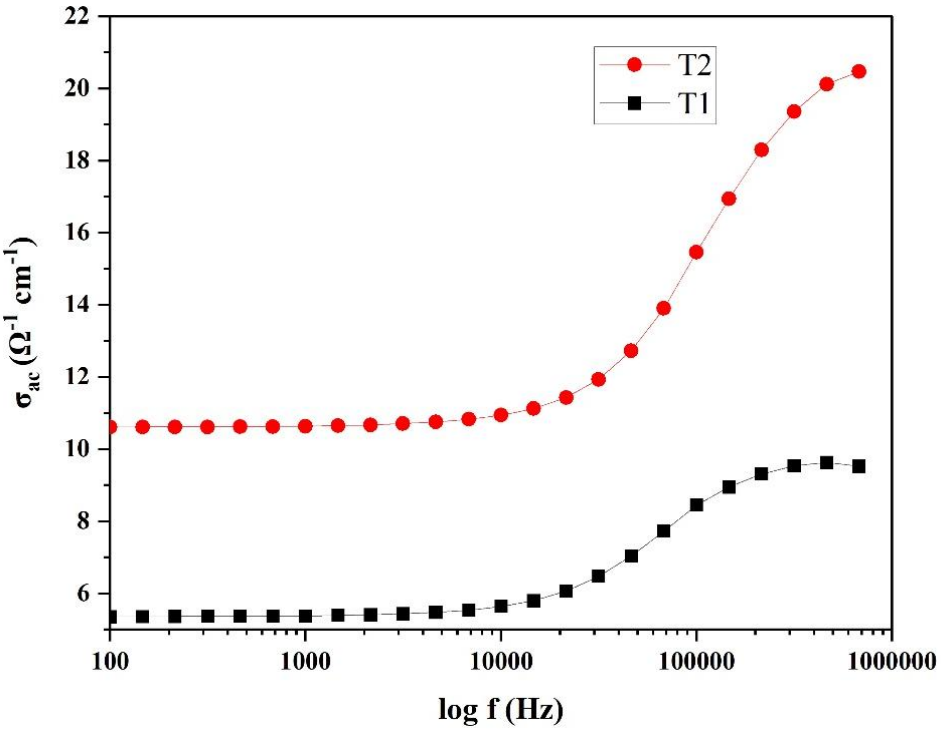

Figure 3.8.1: Ac conductivity of SnO_2 samples T1&T2.

4. CONCLUSION

The SnO_2 nanoparticles were successfully synthesized by solvothermal method by varying the reaction time (3h & 6h). The fabricated nanoparticles were characterized by XRD, SEM, EDAX, FTIR and UV-Vis spectroscopy. The formation of tin oxide has been confirmed by XRD pattern and the crystallite size is calculated using Debye Sherrer formula as 23nm and 27nm. The average size is increased when reaction time is increased. The surface morphology of the samples were studied using scanning electron microscope and both the SnO_2 nanoparticles exhibited spherical morphology. The results of EDX confirms the existence of tin and oxygen. The presence of functional groups were analyzed by FTIR and the strong peaks at 621.42Cm^{-1} and 619.89Cm^{-1} confirms the formation of Sn-O-Sn. Size-dependent optical behavior was demonstrated by optical investigations, which showed that the band gap decreased as reaction time rose. Grain-controlled conduction, frequency-dependent dielectric response, and rising AC conductivity with frequency were all shown by electrical and dielectric experiments. All things considered, the study demonstrates that reaction time is a crucial factor in regulating the structural, optical, and electrical characteristics of SnO_2 nanoparticles, which qualifies them for use in energy storage devices, optoelectronics, and sensors.

REFERENCES

1. George, Nithya S., Lolly Maria Jose, and Arun Aravind. "Review on Transition Metal Oxides and Their Composites for Energy Storage Application." (2022).
2. Deng, Wentao, et al. "Electrochemical capacitors utilising transition metal oxides: an update of recent developments." *Rsc Advances* 1.7 (2011): 1171-1178.

3. Chavali, Murthy S., and Maria P. Nikolova. "Metal oxide nanoparticles and their applications in nanotechnology." *SN applied sciences* 1.6 (2019): 607.

4. Negrescu, Andreea Mariana, et al. "Metal Oxide Nanoparticles: Review of Synthesis, Characterization and Biological Effects." *Journal of Functional Biomaterials* 13.4 (2022): 274.

5. Oskam, Gerko. "Metal oxide nanoparticles: synthesis, characterization and application." *Journal of sol-gel science and technology* 37 (2006): 161-164.

6. Yadav, S., N. Rani, and K. Saini. "A review on transition metal oxides based nanocomposites, their synthesis techniques, different morphologies and potential applications." *IOP Conference Series: Materials Science and Engineering*. Vol. 1225. No. 1. IOP Publishing, 2022.

7. Zhu, Jiping, et al. "Recent progress on nanostructured transition metal oxides as anode materials for lithium-ion batteries." *Journal of Electronic Materials* 51.7 (2022): 3391-3417.

8. Chen, Yao, Xueye Chen, and Yaolong Zhang. "A comprehensive review on metal-oxide nanocomposites for high-performance lithium-ion battery anodes." *Energy & Fuels* 35.8 (2021): 6420-6442.

9. Jeevan, Thevabakthi Siluvai Muthu Arul, et al. "Review on recent progress of nanostructured anode materials for Li-ion batteries." *American Journal of Analytical Chemistry* 13.11 (2022): 431-448.

10. Xie, Haixia, et al. "Solvothermal synthesis of highly crystalline SnO_2 nanoparticles for flexible perovskite solar cells application." *Materials Letters* 234 (2019): 311-314.

11. Yang, Tianye, et al. "Facile synthesis of SnO_2 nanoparticles for improved formaldehyde detection." *New Journal of Chemistry* 42.16 (2018): 13612-13618.

12. Naz, Shaheen, et al. "A simple low cost method for synthesis of SnO_2 nanoparticles and its characterization." *SN Applied Sciences* 2 (2020): 1-8.

13. Karmaoui, Mohamed, et al. "One-step synthesis, structure, and band gap properties of SnO2 nanoparticles made by a low temperature nonaqueous sol–gel technique." *ACS omega* 3.10 (2018): 13227-13238.

14. Chiu, Hui-Chi, and Chen-Sheng Yeh. "Hydrothermal synthesis of SnO_2 nanoparticles and their gas-sensing of alcohol." *The Journal of Physical Chemistry C* 111.20 (2007): 7256-7259.

15. Xiong, Ya, et al. "Defect engineering on SnO_2 nanomaterials for enhanced gas sensing performances." *Advanced Powder Materials* 1.3 (2022): 100033.

16. Yin, Shu, and Takuya Hasegawa. "Morphology control of transition metal oxides by liquid-phase process and their material development." *KONA Powder and Particle Journal* 40 (2023): 94-108.

17. Hermawan, Angga, et al. "One-step synthesis of micro-/mesoporous SnO_2 spheres by solvothermal method for toluene gas sensor." *Ceramics International* 45.12 (2019): 15435-15444.

18. Li, Jian, et al. "Synthesis of tin-glycerate and it conversion into SnO_2 spheres for highly sensitive low-ppm-level acetone detection." *Journal of Materials Science: Materials in Electronics* 31 (2020): 16539-16547.

19. Uddin, Md Tamez, Md Enamul Hoque, and Mitun Chandra Bhoumick. "Facile one-pot synthesis of heterostructure SnO_2/ZnO photocatalyst for enhanced photocatalytic degradation of organic dye." *RSC advances* 10.40 (2020): 23554-23565.

20. Lin, Hwai-En, et al. "A solution-processed tin dioxide film applicable as a transparent and flexible humidity sensor." *RSC advances* 8.53 (2018): 30310-30319.

21. Jung, Eui Hyuk, et al. "Bifunctional surface engineering on SnO_2 reduces energy loss in perovskite solar cells." *ACS Energy Letters* 5.9 (2020): 2796-2801.

22. Karuppiah, Sujatha, et al. "Influence of surfactants on structural, morphological, optical and antibacterial properties of SnO2 nanoparticles." *IET nanobiotechnology* 13.9 (2019): 952-956.

23. Habte, Abebe G., Fekadu Gashaw Hone, and Francis B. Dejene. "Effect of solution pH on structural, optical and morphological properties of SnO_2 nanoparticles." *Physica B: Condensed Matter* 580 (2020): 411832.

24. Karmaoui, Mohamed, et al. "One-step synthesis, structure, and band gap properties of SnO_2 nanoparticles made by a low temperature nonaqueous sol–gel technique." *ACS omega* 3.10 (2018): 13227-13238.

25. Jarvin, M., et al. "A study of the structural, morphological, and optical properties of shock treated SnO_2 nanoparticles: Removal of Victoria blue dye." *Heliyon* 8.6 (2022).

26. Selvakumari, J. Celina, et al. "Structural, morphological, and optical properties of tin (IV) oxide nanoparticles synthesized using Camellia sinensis extract: a green approach." *International Journal of Minerals, Metallurgy, and Materials* 24 (2017): 1043-1051.

27. Kumar, Shalendra, et al. "Tailoring the structural, electronic structure and optical properties of Fe: SnO_2 nanoparticles." *Journal of Electron Spectroscopy and Related Phenomena* 240 (2020): 146934.

28. Khan, Ibrahim, Zain H. Yamani, and Ahsanulhaq Qurashi. "Sonochemical-driven ultrafast facile synthesis of SnO_2 nanoparticles: Growth mechanism structural electrical and hydrogen gas sensing properties." *Ultrasonics sonochemistry* 34 (2017): 484-490.

29. Dhinakar, K. Gnanaprakasam, and S. Meenakshi Sundar. "Structural & optical properties of Co DOPED SnO_2 nanoparticles synthesised by microwave assisted solvothermal method." *IOSR J. Appl. Phys* 3.01 (2017): 92-97.

30. Supin, K. K., et al. "Structural, optical and magnetic properties of pure and 3d metal dopant-incorporated SnO_2 nanoparticles." *RSC advances* 12.41 (2022): 26712-26726.

31. Kumar, Virender, et al. "Effect of solvent on crystallographic, morphological and optical properties of SnO_2 nanoparticles." *Materials Research Bulletin* 85 (2017): 202-208.

32. Habte, Abebe G., Fekadu G. Hone, and Francis B. Dejene. "Influence of annealing temperature on the structural, morphological and optical properties of SnO_2 nanoparticles." *Physica B: Condensed Matter* 580 (2020): 411760.

33. Khan, Sardarali, et al. "Investigation of structural, optical, electrochemical and dielectric properties of SnO_2/GO nanocomposite." *Journal of Materials Science: Materials in Electronics* 30 (2019): 10202-10210.

34. Karthik, K., V. Revathi, and Tetiana Tatarchuk. "Microwave-assisted green synthesis of SnO_2 nanoparticles and their optical and photocatalytic properties." *Molecular Crystals and Liquid Crystals* 671.1 (2018): 17-23.

35. Parthibavarman, M., et al. "Effect of copper on structural, optical and electrochemical properties of SnO_2 nanoparticles." *Journal of optoelectronics and advanced materials* 12.9 (2010): 1894.

36. Shahidi, M. M., et al. "Effect of GLAD technique on optical and electrical properties of SnO_2/Ag/SnO_2 structure." *Infrared Physics & Technology* 106 (2020): 103263.

37. Soumya, S. S. "Optical, dielectric and structural properties of SnO_2 nanoparticles via sol-gel method." *Journal of Physics: Conference Series*. Vol. 2426. No. 1. IOP Publishing, 2023.

38. Khan, Danish, et al. "Improving the optical properties of SnO_2 nanoparticles through Ni doping by sol-gel technique." *Current Research in Green and Sustainable Chemistry* 4 (2021): 100079.

39. Gatea, Hamed A. "Impact of sintering temperature on crystallite size and optical properties of SnO_2 nanoparticles." *Journal of Physics: Conference Series*. Vol. 1829. No. 1. IOP Publishing, 2021.

40. Mehraj, Sumaira, and M. Shahnawaze Ansari. "Structural, electrical and magnetic properties of (Fe, Co) co-doped SnO2 diluted magnetic semiconductor nanostructures." *Physica E: Low-Dimensional Systems and Nanostructures* 65 (2015): 84-92.
41. Soltan, Wissem Ben, et al. "Effect of hydrolysis ratio on structural, optical and electrical properties of SnO2 nanoparticles synthesized by polyol method." *Optical Materials* 58 (2016): 142-150.
42. Divya, J., et al. "Structural, optical, electrical and magnetic properties of Cu and Ni doped SnO2 nanoparticles prepared via Co-precipitation approach." *Physica B: Condensed Matter* 588 (2020): 412169.
43. Singh, Anupinder, et al. "Origin of large dielectric constant with large remnant polarization and evidence of magnetoelectric coupling in multiferroic La modified BiFeO3-PbTiO3 solid solution." *arXiv preprint arXiv:1002.1545* (2010).
44. Chérif, Saïda Fatma, et al. "Ac conductivity, electric modulus analysis, dielectric behavior and Bond Valence Sum analysis of Na3Nb4As3O19 compound." *Arabian Journal of Chemistry* 13.6 (2020): 5627-5638.
45. Dhinakar, K. Gnanaprakasam, et al. "Structural, optical and impedance properties of SnO 2 nanoparticles." *Journal of Materials Science: Materials in Electronics* 27 (2016): 5818-5824.